Acta Crystallographica Section C
Crystal Structure Communications
ISSN 0108-2701

Coordination polymers and hydrogen-bonded assemblies of 2,2′-[2,5-bis-(carboxymethoxy)-1,4-phenylene]-diacetic acid with ammonium, lanthanum and zinc cations

Hatem M. Titi, Anirban Karmakar and Israel Goldberg*

School of Chemistry, Sackler Faculty of Exact Sciences, Tel-Aviv University, Ramat-Aviv, 69978 Tel-Aviv, Israel
Correspondence e-mail: goldberg@post.tau.ac.il

Received 20 July 2010
Accepted 4 August 2010
Online 18 August 2010

We report the synthesis of the 2,2′-[2,5-bis(carboxymethoxy)-1,4-phenylene]diacetic acid ($TALH_4$) ligand and the structures of its adducts with ammonium, namely diammonium 2,2′-[2,5-bis(carboxymethyl)-1,4-phenylenedioxy]diacetate, $2NH_4^+\cdot C_{14}H_{12}O_{10}^{2-}$, (I), lanthanum, namely poly[[aquabis[μ_4-2,2′-(2-carboxylatomethyl-5-carboxymethyl-1,4-phenylenedioxy)-diacetato]dilanthanum(III)] monohydrate], $\{[La_2(C_{14}H_{11}O_{10})_2(H_2O)]\cdot H_2O\}_n$, (II), and zinc cations, namely poly[[{μ_4-2,2′-[2,5-bis(carboxymethyl)-1,4-phenylenedioxy]diacetato}-zinc(II)] trihydrate], $\{[Zn(C_{14}H_{12}O_{10})]\cdot 3H_2O\}_n$, (III), and poly[[diaqua(μ_2-4,4′-bipyridyl){μ_4-2,2′-[2,5-bis(carboxymethyl)-1,4-phenylenedioxy]diacetato}dizinc(II)] dihydrate], $\{[Zn_2(C_{14}H_{10}O_{10})(C_{10}H_8N_2)(H_2O)_2]\cdot 2H_2O\}_n$, (IV), the formation of all four being associated with deprotonation of $TALH_4$. Adduct (I) is a diammonium salt of $TALH_2^{2-}$, with the ions located on centres of crystallographic inversion. Its crystal structure reveals a three-dimensional hydrogen-bonded assembly of the component species. Reaction of $TALH_4$ with lanthanum trinitrate hexahydrate yielded a two-dimensional double-layer coordination polymer, (II), in which the La^{III} cations are nine-coordinate. With zinc dinitrate hexahydrate, $TALH_4$ forms 1:1 two-dimensional coordination polymers, in which every Zn^{II} cation is linked to four neighbouring $TALH_2^{2-}$ anions and each unit of the organic ligand is coordinated to four different tetrahedral Zn^{II} cation connectors. The crystal structure of this compound accommodates molecules of disordered water at the interface between adjacent polymeric layers to give (III), and it has been determined with low precision. Another polymer assembly, (IV), was obtained when zinc dinitrate hexahydrate was reacted with $TALH_4$ in the presence of an additional 4,4′-bipyridyl ligand. In the crystal structure of (IV), the bipyridyl and TAL^{4-} entities are located on two different inversion centres. The ternary coordination polymers form layered arrays with corrugated surfaces, with the Zn^{II} cation connectors revealing a tetrahedral coordination environment. The two-dimensional polymers in (II)–(IV) are interconnected with each other by hydrogen bonds involving the metal-coordinated and noncoordinated molecules of water. $TALH_4$ is doubly deprotonated, $TALH_2^{2-}$, in (I) and (III), triply deprotonated, *viz.* $TALH^{3-}$, in (II), and quadruply deprotonated, *viz.* TAL^{4-}, in (IV). This report provides the first structural characterization of $TALH_4$ (in deprotonated form) and its various supramolecular adducts. It also confirms the potential utility of this tetraacid ligand in the formulation of coordination polymers with metal cations.

Comment

This study is part of our exploratory search for multidentate polycarboxylic acid ligands that can be utilized, in combination with metal cations, in the construction of coordination networks (Goldberg, 2005, 2008). These ligands can be readily deprotonated to balance the charge of the metal cations they interact with (and thus enjoy electrostatic attraction to the metal centres) without the need to incorporate foreign anions into the product. Much current research activity has been directed towards the programmed synthesis of open metal–organic frameworks (MOFs) in view of their potential utility in gas storage (*e.g.* Eddaoudi *et al.*, 2002). Divergent disposition of the carboxylic acid sensor groups substituted on rigid aromatic backbones was found to be a crucial element in the design of microporous solids (Rosi *et al.*, 2005; Eddaoudi *et al.*, 2002). In this context, the present work expands in particular on earlier studies with the tetrafunctional ligand benzene-1,2,4,5-tetracarboxylic acid (*e.g.* Fabelo *et al.*, 2006; Ghosh & Bharadwaj, 2004). We use the same aromatic backbone (the benzene ring) but with longer carboxylic acid substituents, by introducing in 2,2′-[2,5-bis(carboxymethoxy)-1,4-phenylene]diacetic acid ($TALH_4$) $-CH_2-$ and $-OCH_2-$ spacers between the acid groups and the benzene ring. By doing so, our design also imparts some additional conformational flexibility to the organic component, due to the aliphatic nature of the added spacer groups. It was anticipated that the –COOH functions in this ligand may orient in different directions, in and out of the plane of the aromatic core, and thus direct possible coordination to potential metal cation connectors in two and three dimensions to yield $TALH_4$-based robust metal–organic networks and frameworks.

Compound (I) was formed serendipitously, while attempting to coordinate $TALH_4$ to cadmium(II) cations in a mildly basic environment of ammonium hydroxide. It represents a 2:1 NH_4^+–$TALH_2^{2-}$ hydrogen-bonded trimer, with the organic ligand entities located on centres of inversion (Fig. 1). The nearly linear N—H···O hydrogen-bonding interactions are associated with double deprotonation of $TALH_4$, which occurs preferentially on the two more acidic carboxylic acid functions in the carboxymethoxy residues. As a result, the $TALH_2^{2-}$ anion, which bears two carboxylate H-atom acceptors and two carboxylic acid H-atom donor groups, is self-complimentary for hydrogen bonding (Table 1). Correspondingly, every $TALH_2^{2-}$ unit associates *via* O—H···$^-$OOC charge-assisted

  doi:10.1107/S0108270110031318

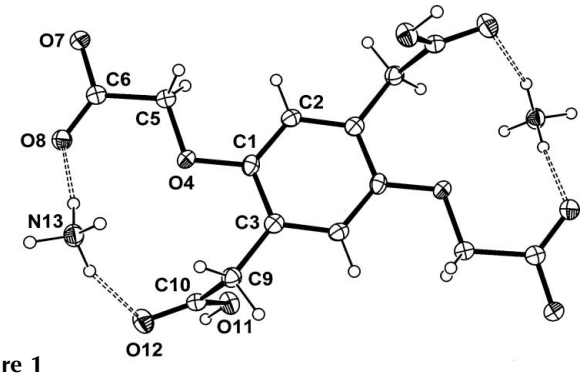

Figure 1
The molecular structure of (I), showing the atom-labelling scheme. The $TALH_2^{2-}$ anions are located on centres of inversion, and only atoms in the asymmetric unit are labelled. Displacement ellipsoids are drawn at the 50% probability level at 110 (2) K and H atoms are shown as small spheres of arbitrary radii. Hydrogen bonds are denoted by dashed lines.

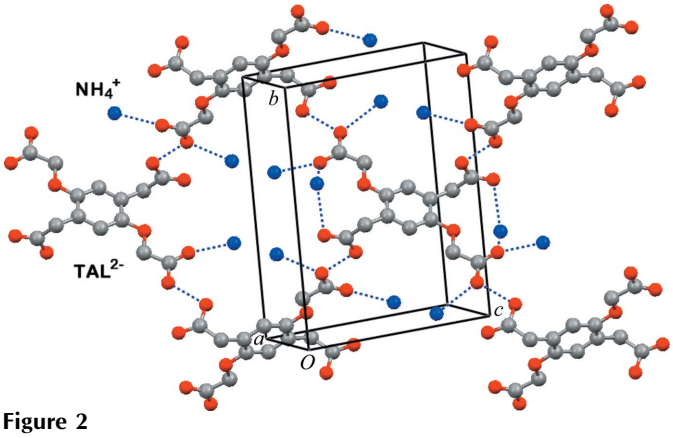

Figure 2
The crystal structure of (I). Intermolecular hydrogen bonds are indicated by dashed lines. Note that the $TALH_2^{2-}$ anion is linked to four neighbouring $TALH_2^{2-}$ anions and six ammonium cations. H atoms have been omitted.

hydrogen bonds with four neighbouring $TALH_2^{2-}$ ligands. In addition, the two carboxylate functions interact *via* $NH_4^+\cdots{}^-OOC$ hydrogen bonds with six adjacent ammonium cations (Fig. 2). The tetrahedral tetradentate functionality of the latter allows it to form hydrogen bonds to two carboxylate functionalities of a given ligand (Fig. 1), as well as to the carboxylate functions of two other ligands (Table 1). The supramolecular charge-assisted hydrogen bonding between the component species extends throughout the crystal structure in three dimensions (Fig. 2). Electrostatic interactions between the charged components further stabilize the three-dimensionally interlinked supramolecular assembly in (I). The structures of ammonium salts of the closely related benzene-1,2,4,5-tetracarboxylic acid reveal similar N—H···O and O—H···O hydrogen-bonding interactions between the component species (Dutkiewicz *et al.*, 2007; Bergstrom *et al.*, 2000; Jessen *et al.*, 1992).

Reaction of lanthanum trinitrate hexahydrate with $TALH_4$ led to the formation of a two-dimensional coordination polymer of 1:1 La^{III}–$TALH^{3-}$ stoichiometry, (II) (Fig. 3). The two crystallographically independent metal cations that form a dinuclear cluster are nine-coordinate (Table 2). Atom La1 coordinates to six carboxylate groups of different $TALH^{3-}$ anions in a monodentate fashion, to another carboxylate group in a bidentate fashion, and also to the ether O-atom site

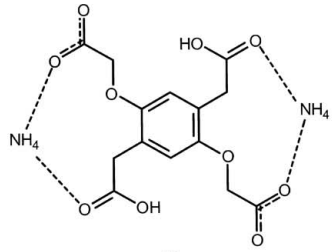

(I)

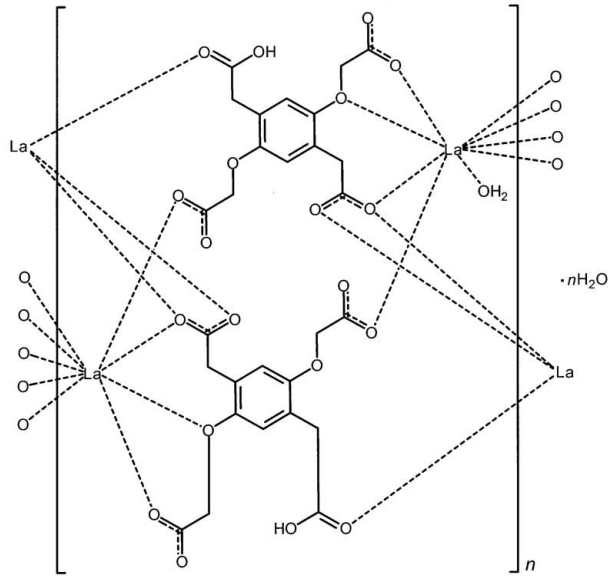

(II)

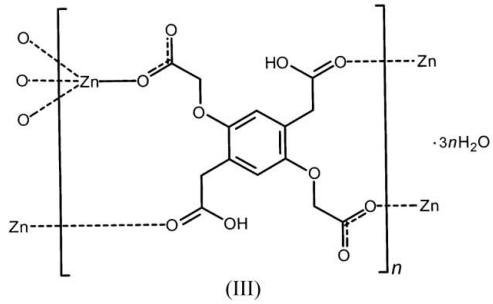

(III)

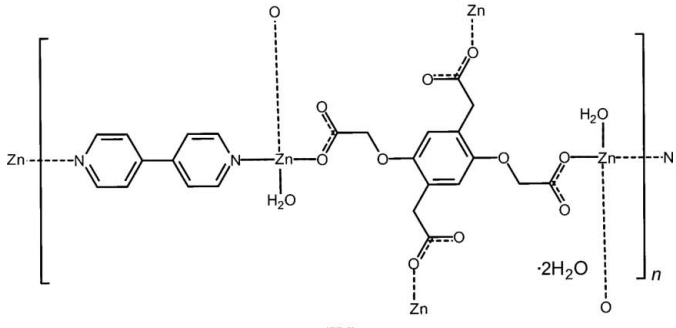

(IV)

of one of the ligands. Atom La2 coordinates to five carboxylate groups of adjacent $TALH^{3-}$ anions in a monodentate fashion, to another carboxylate group in a bidentate

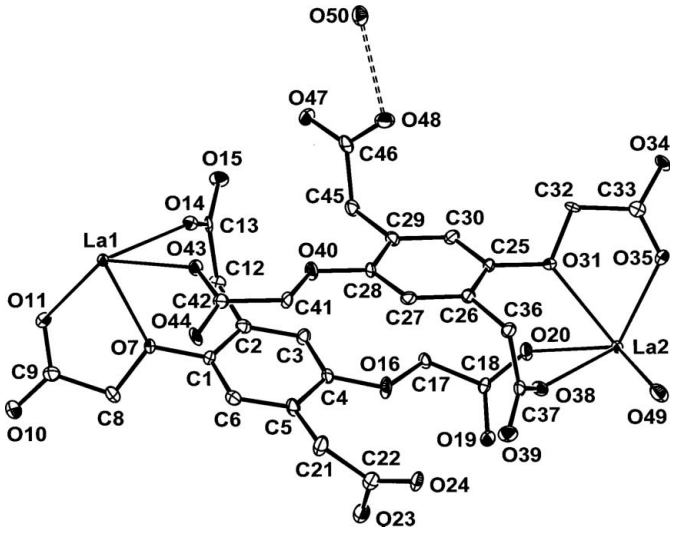

Figure 3
The asymmetric unit of (II), showing the atom-labelling scheme. Displacement ellipsoids are drawn at the 50% probability level at 110 (2) K. The hydrogen bond is denoted by a double dashed line. H atoms have been omitted.

fashion, to an ether O-atom site of one of the ligands, and finally to a water molecule (Table 2). In the resulting coordination network, adjacent La^{III} cations (whether within the dinuclear cluster or between clusters) are bridged by several organic ligands. This leads to the formation of robust polymeric arrays which extend parallel to the $(\bar{1}01)$ plane of the crystal structure, in which the $TALH^{3-}$ components are arranged in two layers, due to the multiple coordination capacity of the inorganic connectors and the spatial disposition of their coordination valencies (Fig. 4). The layered assemblies have corrugated surfaces lined with the metal-coordinated water molecules and the –COOH residues. In the crystal structure, the double-layer polymeric networks are held together by an extensive array of O—H···O hydrogen bonds, which involves the H atoms of the metal-coordinated water ligand O49, the carboxylic acid functions OH23 and OH48, and the noncoordinated water molecules O50 trapped in the structure (Table 3). The observed multiple coordination pattern of the oxophilic La^{III} cations to carboxylic acid/carboxylate/water ligands, with La—O bond lengths in the range 2.4–2.7 Å, is similar to earlier documented findings in polymeric networks incorporating La^{3+} cations and deprotonated pyrromellitic acid anions (Wen *et al.*, 2004; Chui *et al.*, 2001; Wu *et al.*, 1996).

A similar reaction between the tetraacid ligand and a zinc salt also resulted in the formation of a coordination polymer with two-dimensional connectivity, (III) (Fig. 5). In the layered arrays, rows of the $TALH_2^{2-}$ ligand alternate with rows of the Zn^{II} cation connectors in both directions (Fig. 6). The latter are characterized by a tetrahedral coordination environment, linking in a monodentate manner to the carboxylate/carboxylic acid groups of four neighbouring ligands (Table 4). Each pair of neighbouring Zn^{II} cations in the layer is bridged by two ligand anions. The layered arrays are oriented perpendicular to the *b* axis of the crystal, being centred at $y = \frac{1}{4}$ and $\frac{3}{4}$. Although the Zn^{II} cation connectors are characterized by a tetrahedral coordination geometry, the observed coordination pattern is limited to two dimensions, the coordination directionality of the Zn^{II} cations not being matched by a complimentary spatial disposition of the COO/COOH ligating sites in the organic ligand. Rather, the adapted conformation of the aliphatic arms in $TALH_2^{2-}$ minimizes the empty space within the coordinated layer (Fig. 6). Noncoordinated water molecules are intercalated between the coordination layers in zones centred at $y = 0$ and $\frac{1}{2}$, and form hydrogen bonds between them. However, due to the poor quality of the crystals, associated with severe disorder of the crystallization solvent, these interactions could not be characterized reliably. The low quality of the diffraction data in this case is also

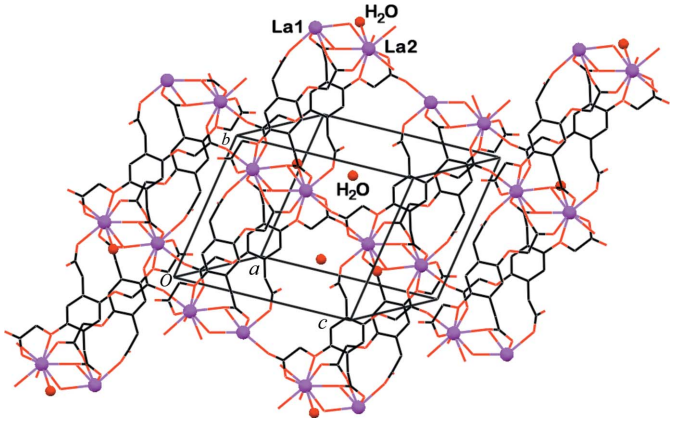

Figure 4
A view of the layered coordination polymer in (II), aligned parallel to the $(\bar{1}01)$ plane of the crystal structure, along with the noncoordinated molecules of water located in the interstitial voids. The La^{III} cations and water molecules in the otherwise wireframe illustration are denoted by small spheres.

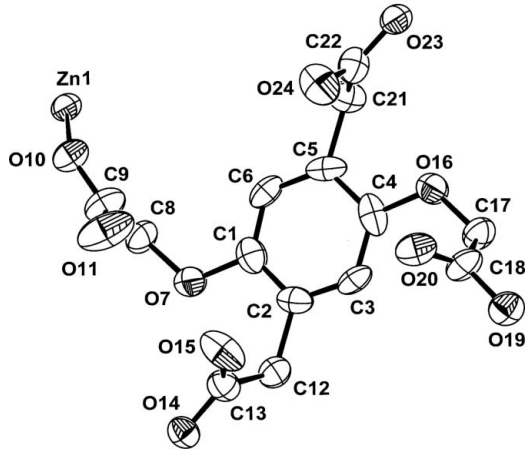

Figure 5
The asymmetric unit of (III), showing the atom-labelling scheme. Displacement ellipsoids are drawn at the 50% probability level at 110 (2) K. H atoms have been omitted. Note the large-amplitude atomic displacement parameters, possibly indicating some orientational disorder of the organic ligand in this structure.

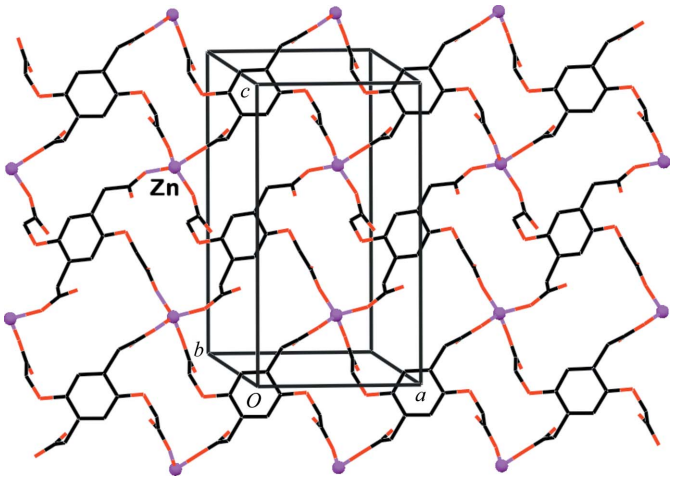

Figure 6
A face-on view of the layered coordination polymer in (III), aligned perpendicular to the *b* axis of the crystal structure. The disordered molecules of water located in the interfacial zones between neighbouring polymers are not shown. The Zn^{II} cations are depicted as small spheres.

affected by possible orientational in-layer disorder of the $TALH_2^{2-}$ anions, which have a nearly square shape and a similar coordination environment in the four lateral directions. Considering also the loose packing of the layers along the normal axis, a random interchange between the positions of the $-CH_2COO/-CH_2COOH$ and $-OCH_2COO/-OCH_2COOH$ groups (the H atoms of these fragments could not be located) in selected/fault sites of the crystal structure cannot be excluded.

Zinc cations are known to be well coordinated by ligands with both O- and N-ligating sites. Correspondingly, on addition of the 4,4′-bipyridyl reagent (bpy) to the reaction mixture of zinc dinitrate and $TALH_4$, the two ligands may compete for coordination sites on the metal core. Indeed, compound (IV) represents a ternary product of 2:1:1 Zn^{II}–TAL^{4-}–bpy stoichiometry (Fig. 7), where the two multidentate organic linkers (which reside on two different inversion centres) are coordinated to the metal. The Zn^{II} cation connectors reveal a tetrahedral coordination geometry, each associated with the carboxylate groups of two neighbouring TAL^{4-} anions (in a

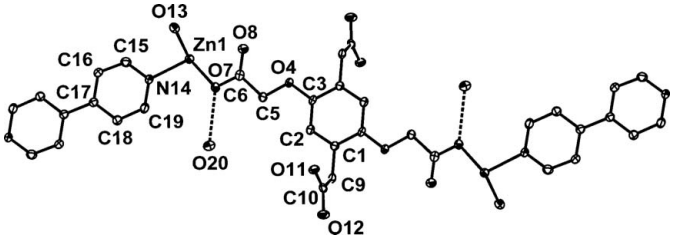

Figure 7
Part of the structure of (IV), showing the atom-labelling scheme. The TAL^{4-} anion and bpy ligand are located on centres of inversion, and only atoms in the asymmetric unit are labelled. Displacement ellipsoids are drawn at the 50% probability level at 110 (2) K. Hydrogen bonds to noncoordinated water molecules are denoted by dashed lines. H atoms have been omitted.

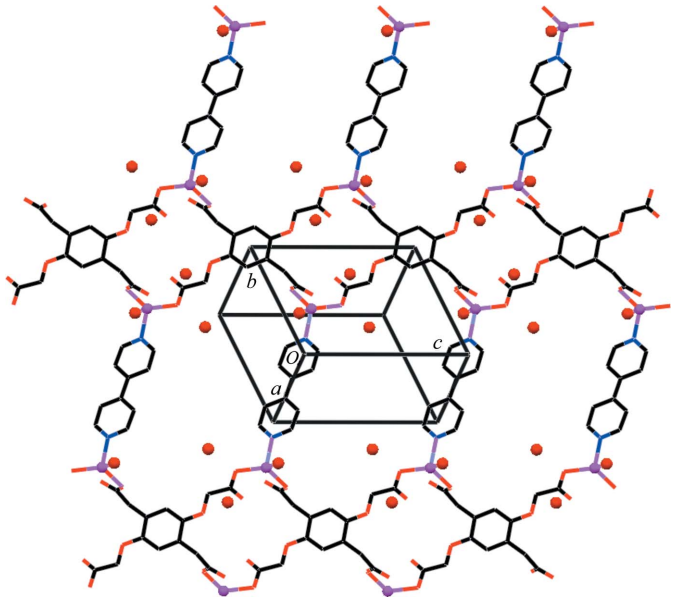

Figure 8
The layered ternary coordination polymer in (IV). The Zn^{II} cations and water molecules are indicated by small spheres. Note that the metal-bound water ligands are oriented in an alternating manner (either up or down) perpendicular to the layered arrays. The noncoordinated water molecules occupy interstitial voids within and between the layers.

monodentate mode), the N-atom site of the bpy ligand and a molecule of water (Table 5). The TAL^{4-} tetraanion is linked simultaneously in the lateral directions to four different Zn^{II} cations, while the bidentate bpy ligand bridges two Zn^{II} cation nodes. As illustrated in Fig. 8, this results in the formation of two-dimensional coordination networks aligned parallel to the (210) plane of the crystal structure. The metal-bound water ligands are oriented perpendicular to the network mean plane in alternating directions. The thin shape of the bpy linkers in the grid networks creates open voids between them, which are penetrated from above and below by the O13 metal-bound water ligands of adjacent layers. In addition, noncoordinated water species O20 are accommodated between the layers. The two water molecules form bridges by hydrogen bonding between the interpentrating coordination networks (Table 6).

Coordination polymers sustained by zinc–carboxylate coordination synthons are abundant in the literature. The observed Zn—O and Zn—N coordination distances (Tables 4 and 5) are in the normally expected ranges for such polymeric compounds, as confirmed by a survey of the Cambridge Structural Database (CSD, Version 5.31, May 2010 update; Allen, 2002). Among these related polymeric compounds, recent references to zinc–pyromellitate coordination compounds (Lu *et al.*, 2005; Wang *et al.*, 2007) and to those also incorporating the bpy ligand (Wu *et al.*, 2001; Huang *et al.*, 2009) are of particular relevance.

In summary, we have reported here the synthesis of a new tetracarboxylic acid ligand, $TALH_4$, and demonstrated its capacity to form coordination networks with metal cations. In spite of the conformational flexibility imparted to this ligand by inserting aliphatic spacers between the aromatic core and

the four diverging –COOH groups, the formation of only two-dimensional coordination polymers has been observed so far. However, the coordination polymerization in (II)–(IV) is supplemented by hydrogen-bonding interactions along the third dimension.

Experimental

The tetraacid ligand was obtained *via* a three-step procedure. First, commercially available 2,5-dihydroxybenzene-1,4-diacetic acid (0.5 g, 2.21 mmol) was dissolved in absolute EtOH (50 ml), sulfuric acid (4 ml) was added dropwise, and the mixture was refluxed overnight. The solution was then evaporated and extracted with dichloromethane. The organic extracts were collected over anhydrous sodium sulfate. Subsequent removal of the solvent gave the diethyl 2,2′-(2,5-dihydroxy-1,4-phenylene)diacetate intermediate, *A*, in 85% yield. In the second step, a mixture of *A* (450 mg, 4.6 mmol), methyl bromoacetate (520 mg, 3.4 mmol) and potassium carbonate (630 mg, 4.6 mmol) was dissolved in acetone (50 ml) and refluxed for 5 h at 333 K. The resulting mixture was filtered and the residue dissolved in water to remove unreacted potassium carbonate. Intermediate *B*, namely 2,2′-[2,5-bis(2-methoxy-2-oxoethoxy)-1,4-phenylene]diacetate, was isolated by filtration and dried *in vacuo* (yield 61%). It was then dissolved in methanol (20 ml), 5 *N* NaOH (3 ml) was added, and the mixture was refluxed overnight. After removal of the reaction solvent by evaporation, the crude product was treated with 0.5 *N* HCl, washed with water and dried *in vacuo*, yielding a white precipitate (in 72% yield) as the final tetraacid product 2,2′-[2,5-bis-(carboxymethoxy)-1,4-phenylene]diacetic acid ($TALH_4$). ^{1}H NMR (DMSO-d^6): δ 12.53 (*bs*, 4H, –COOH), 6.81 (*s*, 2H, Ar—H), 4.56 (*s*, 4H, $-OCH_2$), 3.53 (*s*, 4H, $-CH_2$).

Compound (I) was obtained by dissolving $TALH_4$ (5 mg, 0.015 mmol) and cadmium dinitrate tetrahydrate (9 mg, 0.03 mmol) in water (4 ml), along with a few drops of ammonium hydroxide to assist in the deprotonation of $TALH_4$. The mixture was heated for 2 d in a bath reactor at 353 K, to yield colourless crystals of (I) after gradual cooling to room temperature. It turned out that, under the given experimental conditions, the cadmium cations did not react with $TALH_4$, and instead the diammonium salt of the acid was formed. FT–IR (KBr, ν, cm^{-1}): 2963 (*bs*), 1716 (*s*), 1525 (*s*), 1416 (*s*), 1340 (*b*), 1301 (*b*), 1218 (*b*), 1158 (*b*), 1091 (*s*), 896 (*b*), 721 (*s*), 678 (*s*), 628 (*s*), 564 (*s*), 441 (*s*).

Compound (II) was obtained by dissolving $TALH_4$ (3.3 mg, 0.01 mmol) and lanthanum trinitrate hexahydrate (8.2 mg, 0.02 mmol) in water (7 ml). This solution was placed in a sealed and tightly capped vessel, which was heated for 2 d at 393 K in a bath reactor. Colourless crystals of (II) precipitated in the reactor. FT–IR (KBr, ν, cm^{-1}): 3419 (*bs*), 2925 (*s*), 1584 (*s*), 1512 (*s*), 1391 (*s*), 1335 (*s*), 1210 (*s*), 1053 (*s*), 645 (*bs*).

In a similar procedure, $TALH_4$ (20 mg, 0.06 mmol) and zinc dinitrate hexahydrate (30 mg, 0.12 mmol) were dissolved in a 2:1:1 MeOH–DMF–water mixture (DMF is dimethylformamide) (4 ml) and heated for 2 d in a bath reactor at 373 K, yielding (III) as a colourless crystalline product. FT–IR (KBr, ν, cm^{-1}): 3193 (*bs*), 1610 (*s*), 1511 (*s*), 1403 (*s*), 1306 (*s*), 1270 (*s*), 1207 (*s*), 1083 (*s*), 943 (*s*), 788 (*s*), 703 (*s*), 649 (*s*), 608 (*s*).

In another experiment, $TALH_4$ (10 mg, 0.03 mmol), zinc dinitrate hexahydrate (18 mg, 0.06 mmol) and 4,4′-bipyridyl (5 mg, 0.03 mmol) were dissolved in a 6:2:1 MeOH–DMF–water mixture (4.5 ml). After heating the mixture for 2 d in a bath reactor at 373 K, followed by slow evaporation at room temperature for two weeks, X-ray quality colourless crystals of compound (IV) were obtained. FT–IR (KBr, ν, cm^{-1}): 3392 (*bs*), 1602 (*s*), 1388 (*s*), 1216 (*s*), 1077 (*s*), 733 (*s*).

Compound (I)

Crystal data

$2NH_4^+\cdot C_{14}H_{12}O_{10}^{2-}$
M_r = 376.32
Monoclinic, $P2_1/n$
a = 4.8188 (3) Å
b = 14.6889 (8) Å
c = 11.2087 (8) Å
β = 91.855 (2)°
V = 792.97 (9) Å^3
Z = 2
Mo $K\alpha$ radiation
μ = 0.14 mm^{-1}
T = 110 K
0.40 × 0.15 × 0.15 mm

Data collection

Nonius KappaCCD area-detector diffractometer
9862 measured reflections
1598 independent reflections
1243 reflections with $I > 2\sigma(I)$
R_{int} = 0.051

Refinement

$R[F^2 > 2\sigma(F^2)]$ = 0.043
$wR(F^2)$ = 0.102
S = 1.04
1598 reflections
148 parameters
Only H-atom coordinates refined
$\Delta\rho_{max}$ = 0.27 e Å^{-3}
$\Delta\rho_{min}$ = −0.22 e Å^{-3}

Compound (II)

Crystal data

$[La_2(C_{14}H_{11}O_{10})_2(H_2O)]\cdot H_2O$
M_r = 992.31
Triclinic, $P\overline{1}$
a = 10.2508 (2) Å
b = 11.1655 (3) Å
c = 14.7606 (4) Å
α = 79.5944 (12)°
β = 82.1510 (12)°
γ = 69.9402 (17)°
V = 1555.74 (7) Å^3
Z = 2
Mo $K\alpha$ radiation
μ = 2.81 mm^{-1}
T = 110 K
0.15 × 0.15 × 0.10 mm

Data collection

Nonius KappaCCD area-detector diffractometer
Absorption correction: multi-scan (Blessing, 1995)
T_{min} = 0.678, T_{max} = 0.766
25631 measured reflections
6850 independent reflections
5610 reflections with $I > 2\sigma(I)$
R_{int} = 0.062

Refinement

$R[F^2 > 2\sigma(F^2)]$ = 0.037
$wR(F^2)$ = 0.089
S = 1.03
6850 reflections
470 parameters
H-atom parameters constrained
$\Delta\rho_{max}$ = 1.69 e Å^{-3}
$\Delta\rho_{min}$ = −1.78 e Å^{-3}

Compound (III)

Crystal data

$[Zn(C_{14}H_{12}O_{10})]\cdot 3H_2O$
M_r = 459.65
Monoclinic, $P2_1/c$
a = 8.9186 (4) Å
b = 12.2656 (7) Å
c = 16.3199 (8) Å
β = 91.384 (4)°
V = 1784.75 (16) Å^3
Z = 4
Mo $K\alpha$ radiation
μ = 1.45 mm^{-1}
T = 110 K
0.30 × 0.10 × 0.10 mm

Data collection

Nonius KappaCCD area-detector diffractometer
Absorption correction: multi-scan (Blessing, 1995)
T_{min} = 0.675, T_{max} = 0.871
15967 measured reflections
3624 independent reflections
2367 reflections with $I > 2\sigma(I)$
R_{int} = 0.078

Table 1
Hydrogen-bond geometry (Å, °) for (I).

D—H···A	D—H	H···A	D···A	D—H···A
O11—H11···O7^{i}	0.99 (2)	1.52 (2)	2.5123 (19)	175 (2)
N13—H13A···O7^{ii}	0.93 (3)	1.89 (3)	2.822 (2)	178 (2)
N13—H13B···O8	0.93 (3)	1.85 (3)	2.771 (2)	171 (2)
N13—H13C···O12	0.96 (3)	2.05 (3)	2.963 (2)	160 (2)
N13—H13D···O8^{iii}	0.96 (3)	2.10 (3)	3.043 (2)	167 (2)

Symmetry codes: (i) $-x+\frac{1}{2}, y-\frac{1}{2}, -z+\frac{1}{2}$; (ii) $x+\frac{1}{2}, -y+\frac{1}{2}, z+\frac{1}{2}$; (iii) $x+1, y, z$.

Table 2
Selected bond lengths (Å) for (II).

La1—O44^{i}	2.417 (3)	La2—O20	2.450 (3)
La1—O14	2.519 (3)	La2—O34^{iii}	2.486 (3)
La1—O19^{ii}	2.525 (3)	La2—O38	2.509 (3)
La1—O24^{ii}	2.525 (3)	La2—O49	2.524 (3)
La1—O43	2.536 (3)	La2—O35	2.543 (3)
La1—O11	2.540 (3)	La2—O47^{iv}	2.546 (3)
La1—O38^{ii}	2.579 (3)	La2—O15^{iv}	2.625 (3)
La1—O7	2.619 (3)	La2—O14^{iv}	2.638 (3)
La1—O39^{ii}	2.661 (3)	La2—O31	2.718 (3)
La1···La2^{ii}	4.2365 (3)		

Symmetry codes: (i) $-x, -y, -z$; (ii) $x, y-1, z$; (iii) $-x+1, -y+1, -z+1$; (iv) $x, y+1, z$.

Table 3
Hydrogen-bond geometry (Å, °) for (II).

D—H···A	D—H	H···A	D···A	D—H···A
O23—H23···O11^{iv}	1.00	1.60	2.593 (4)	174
O48—H48···O50	0.84	1.68	2.522 (5)	179
O49—H49A···O10^{v}	0.79	1.96	2.710 (5)	158
O49—H49B···O43^{iv}	0.81	2.00	2.797 (4)	170
O50—H50A···O19^{vi}	0.91	1.95	2.839 (4)	164
O50—H50B···O35^{ii}	0.90	1.86	2.753 (4)	171

Symmetry codes: (ii) $x, y-1, z$; (iv) $x, y+1, z$; (v) $x+1, y+1, z$; (vi) $x+1, y-1, z$.

Refinement

$R[F^2 > 2\sigma(F^2)]$ = 0.073	226 parameters
$wR(F^2)$ = 0.220	H-atom parameters constrained
S = 1.08	$\Delta\rho_{max}$ = 1.33 e Å^{-3}
3624 reflections	$\Delta\rho_{min}$ = −0.57 e Å^{-3}

Compound (IV)

Crystal data

$[Zn_2(C_{14}H_{10}O_{10})(C_{10}H_8N_2)(H_2O)_2]\cdot 2H_2O$	β = 94.915 (3)°
M_r = 697.24	γ = 92.412 (3)°
Triclinic, $P\overline{1}$	V = 651.01 (6) Å^3
a = 7.7218 (4) Å	Z = 1
b = 8.3520 (5) Å	Mo $K\alpha$ radiation
c = 10.7204 (6) Å	μ = 1.92 mm^{-1}
α = 108.621 (3)°	T = 110 K
	0.20 × 0.10 × 0.10 mm

Data collection

Nonius KappaCCD area-detector diffractometer	7281 measured reflections
	2794 independent reflections
Absorption correction: multi-scan (Blessing, 1995)	2330 reflections with $I > 2\sigma(I)$
T_{min} = 0.700, T_{max} = 0.831	R_{int} = 0.059

Table 4
Selected bond lengths (Å) for (III).

Zn1—O23^{i}	1.929 (4)	Zn1—O14^{iii}	1.948 (4)
Zn1—O19^{ii}	1.931 (4)	Zn1—O10	1.962 (4)

Symmetry codes: (i) $x-1, y, z$; (ii) $x-1, -y+\frac{1}{2}, z+\frac{1}{2}$; (iii) $x, -y+\frac{1}{2}, z+\frac{1}{2}$.

Table 5
Selected bond lengths (Å) for (IV).

Zn1—O7	1.957 (2)	Zn1—O13	1.988 (2)
Zn1—O11^{i}	1.983 (2)	Zn1—N14	2.073 (3)

Symmetry code: (i) $x, y, z+1$.

Table 6
Hydrogen-bond geometry (Å, °) for (IV).

D—H···A	D—H	H···A	D···A	D—H···A
O13—H13A···O8^{ii}	0.87	1.81	2.676 (3)	172
O13—H13B···O20^{iii}	1.00	1.65	2.632 (3)	164
O20—H20A···O7	0.90	1.82	2.714 (3)	179
O20—H20B···O12^{iv}	0.90	1.85	2.753 (3)	180

Symmetry codes: (ii) $-x+1, -y, -z+1$; (iii) $-x+1, -y+1, -z+1$; (iv) $-x+2, -y+1, -z$.

Refinement

$R[F^2 > 2\sigma(F^2)]$ = 0.048	190 parameters
$wR(F^2)$ = 0.092	H-atom parameters constrained
S = 1.07	$\Delta\rho_{max}$ = 0.48 e Å^{-3}
2794 reflections	$\Delta\rho_{min}$ = −0.71 e Å^{-3}

In (I), the atomic coordinates of all the H atoms, initially included in calculated positions or located in difference Fourier maps, were refined, but with U_{iso}(H) = 1.2U_{eq}(C) for H atoms bound to C atoms, and with U_{iso}(H) = 1.5U_{eq}(O,N) for H atoms bound to O and N atoms. In compounds (II)–(IV), H atoms bound to C atoms were included in calculated positions and constrained to ride on their parent atoms, with C—H = 0.95 and 0.99 Å and with U_{iso}(H) = 1.2U_{eq}(C). Those bound to O atoms were either located in difference Fourier maps or placed in calculated positions to correspond to idealized hydrogen-bonding geometries, with O—H = 0.79–1.00 Å. Their atomic positions were not refined, and they were constrained to ride on their parent atoms, with U_{iso}(H) = 1.5U_{eq}(O).

Compound (III) is a trihydrate of a 1:1 zinc–$TALH_2^{2-}$ adduct. It could be readily recognized by inspection of the difference Fourier map that the water molecules form hydration layers at the interface between the coordination networks. However, they were found to be severely disordered and could not be reliably modelled as discrete O and H atoms. Their contribution to the diffraction pattern was subtracted using the SQUEEZE procedure in *PLATON* (Spek, 2009). The total solvent-accessible void volume and the residual electron-density count in the unit cell were assessed by *PLATON* to be 270 Å^3 and 86 e, respectively, which may correspond approximately to the presence of nearly three water molecules in the asymmetric unit, although independent evidence to this end could not be obtained. Moreover, the atoms of the $TALH_2^{2-}$ anion exhibit large-amplitude in-plane atomic displacement parameters, and the H atoms of the –COOH residues could not be located. The disordered water solvent and these two H atoms have been included in the chemical formula and all values derived from it. The maximum

residual electron-density peaks in (III) are near the peripheral aliphatic arms: 1.33 e Å^{-3} at (0.036, 0.351, 0.631) and 1.01 e Å^{-3} at (0.045, 0.355, 0.294). Correspondingly, the structure of this product could not be determined with high precision comparable with that of structures (I), (II) and (IV). It was included in this report for the sake of completeness.

Five residual peaks above 1.0 e Å^{-3} were found in (II) near the aliphatic fragments and water species: 1.69 e Å^{-3} at (0.426, 0.456, 0.424), 1.67 e Å^{-3} at (0.468, 0.787, 0.028), 1.56 e Å^{-3} at (0.305, 0.059, 0.039), 1.49 e Å^{-3} at (0.460, 0.822, 0.099) and 1.47 e Å^{-3} at (0.251, 0.301, 0.698).

For all four compounds, data collection: *COLLECT* (Nonius, 1999); cell refinement: *DENZO* (Otwinowski & Minor, 1997); data reduction: *DENZO*; program(s) used to solve structure: *SIR97* (Altomare *et al.*, 1994); program(s) used to refine structure: *SHELXL97* (Sheldrick, 2008); molecular graphics: *ORTEPIII* (Burnett & Johnson, 1996) and *Mercury* (Macrae *et al.*, 2006); software used to prepare material for publication: *SHELXL97*.

This research was supported by the Israel Science Foundation (grant No. 502/08).

Supplementary data for this paper are available from the IUCr electronic archives (Reference: SU3049). Services for accessing these data are described at the back of the journal.

References

Allen, F. H. (2002). *Acta Cryst.* B**58**, 380–388.

Altomare, A., Cascarano, G., Giacovazzo, C., Guagliardi, A., Burla, M. C., Polidori, G. & Camalli, M. (1994). *J. Appl. Cryst.* **27**, 435.

Bergstrom, C. L., Luck, R. L. & Luehrs, D. C. (2000). *Acta Cryst.* C**56**, e591.

Blessing, R. H. (1995). *Acta Cryst.* A**51**, 33–38.

Burnett, M. N. & Johnson, C. K. (1996). *ORTEPIII*. Report ORNL-6895. Oak Ridge National Laboratory, Tennessee, USA.

Chui, S. S.-Y., Siu, A., Feng, X., Zhang, Z. Y., Mak, T. C. W. & Williams, I. D. (2001). *Inorg. Chem. Commun.* **4**, 467–470.

Dutkiewicz, G., Borowiak, T., Pietraszkiewicz, M. & Pietraszkiewicz, O. (2007). *Acta Cryst.* E**63**, o4101.

Eddaoudi, M., Kim, J., Rosi, N. L., Vodak, D., Wachter, J., O'Keeffe, M. & Yaghi, O. M. (2002). *Science*, **295**, 469–472.

Fabelo, O., Canadillas-Delgado, L., Pasan, J., Ruiz-Perez, C. & Julve, M. (2006). *CrystEngComm*, **8**, 338–345.

Ghosh, S. K. & Bharadwaj, P. K. (2004). *Inorg. Chem.* **43**, 5180–5182.

Goldberg, I. (2005). *Chem. Commun.* pp. 1243–1254.

Goldberg, I. (2008). *CrystEngComm*, **10**, 637–645.

Huang, S.-H., Lin, C.-H., Wu, W.-C. & Wang, S.-L. (2009). *Angew. Chem. Int. Ed.* **48**, 6124–6127.

Jessen, S. M., Kuppers, M. & Luehrs, D. C. (1992). *Z. Naturforsch. Teil B*, **47**, 1141–1153.

Lu, K.-L., Chen, Y.-F., Cheng, Y.-W., Liao, R.-T., Liu, Y.-H. & Wen, Y. S. (2005). *Cryst. Growth Des.* **5**, 403–405.

Macrae, C. F., Edgington, P. R., McCabe, P., Pidcock, E., Shields, G. P., Taylor, R., Towler, M. & van de Streek, J. (2006). *J. Appl. Cryst.* **39**, 453–457.

Nonius (1999). *COLLECT*. Nonius BV, Delft, The Netherlands.

Otwinowski, Z. & Minor, W. (1997). *Methods in Enzymology*, Vol. 276, *Macromolecular Crystallography*, Part A, edited by C. W. Carter Jr & R. M. Sweet, pp. 307–326. New York: Academic Press.

Rosi, N. L., Kim, J., Eddaoudi, M., Chen, B., O'Keeffe, M. & Yaghi, O. M. (2005). *J. Am. Chem. Soc.* **127**, 1504–1518.

Sheldrick, G. M. (2008). *Acta Cryst.* A**64**, 112–122.

Spek, A. L. (2009). *Acta Cryst.* D**65**, 148–155.

Wang, J., Lu, L., Yang, B., Zhao, B.-Z. & Ng, S. W. (2007). *Acta Cryst.* E**63**, m2986.

Wen, Y.-H., Zhang, J., Li, Z.-J., Qin, Y.-Y., Kang, Y., Hu, R.-F., Cheng, J.-K. & Yao, Y.-G. (2004). *Acta Cryst.* E**60**, m535–m537.

Wu, C.-D., Lu, C.-Z., Wu, D.-M., Zhuang, H.-H. & Huang, J.-S. (2001). *Inorg. Chem. Commun.* **4**, 561–564.

Wu, L. P., Munakata, M., Yamamoto, M., Kuroda-Sowa, T. & Maekawa, M. (1996). *J. Coord. Chem.* **37**, 361–369.